

Cite this: *CrystEngComm*, 2012, 14, 5572–5578

www.rsc.org/crystengcomm

PAPER

Spray drying mass-production route for Mg-doped LiNbO₃ (Mg:LN) polycrystalline powder based on a wet-chemical method

Qingbo Liu,^a Dehui Sun,^a Tao Yan,^a Feifei Zheng,^b Yunhua Sang,^a Hong Liu,^{*a} Jiyang Wang^a and Tadashi Ohachi^c

Received 23rd February 2012, Accepted 28th May 2012

DOI: 10.1039/c2ce25262g

A mass production route for Mg-doped LiNbO₃ (Mg:LN) polycrystalline powder was proposed based on a wet-chemical method/spray drying process. A stable homogenous precursor solution was prepared by dissolving commercial Nb(OH)₅, Li₂CO₃ and MgO, and was stabilized with citric acid (CA) as a chelating agent. Spherical Mg:LN precursor powder can be obtained by a spray-drying method, and spherical mono-phase perovskite Mg:LN polycrystalline powder with uniform size was obtained by calcining the precursor powder at relatively low temperature. Thermogravimetry–differential thermal analysis (TG–DTA), X-ray diffraction (XRD), infrared spectroscopy and scanning electron microscopy (SEM) were used to characterize the precursor and product powder. The as-obtained Mg:LN powder was used for Mg:LN single-crystal growth. The obtained Mg:LN single crystal possesses both high optical homogeneity and ingredient uniformity. This mass production route for preparation of Mg:LN powder provides a solution to the problem of defects in Mg:LN single crystals caused by nonhomogeneity of magnesium distribution.

1. Introduction

LiNbO₃ (LN) is a very important multifunctional material, which can be used in fields of electronic and optics due to its nonlinear optical¹ electro-optic,² ferroelectric,^{3,5} and dielectric properties.^{4,6} The application of LN crystals is very extensive, in areas such as optical signal processing,⁷ holographic recording,^{8,9} optical waveguides,¹⁰ optical demultiplexers,¹¹ self-frequency doubled lasers,¹² optical parametric oscillators (OPOs)¹³ and surface acoustic wave (SAW) devices.^{14–16} Available commercial LN crystals are usually grown from a melt with congruent composition (Li/Nb ratio = 48.6/51.4) by the traditional Czochralski method.¹⁷ The congruent LiNbO₃ (CLN) has high optical quality and composition uniformity, however, some intrinsic defects such as Li-vacancies and Nb_{Li} (antisites Nb at Li sites)^{18–20} diminish its optimal properties, such as nonlinear optical property, and photodamage resistance property²¹ which influences the stability of optical devices when irradiated with high-power laser beams. The main constraint for the optical application of CLN lies in the low optical damage resistance ability. Many efforts have been attempted to reduce the optical damage in CLN with doping by MgO,^{22–24} and Bryan *et al.*²⁵ have reported that the MgO doping concentration around 4.5–5.0 mol% obviously improved optical damage resistance ability.

MgO-doped LN (Mg:LN) crystals have received much attention over many years. Homogeneous and high purity Mg:LN powders are essential for the growth of high quality crystals with excellent physical and chemical properties. Conventionally, Mg:LN powder is synthesized *via* a solid-state reaction process by mixing the raw material powders, such as MgO, LiCO₃ and Nb₂O₅, and calcining at a high temperature (>1100 °C). This high temperature involved in the reaction process leads to composition deviation from original stoichiometry due to lithium evaporation.^{26–29} It is difficult to obtain a Mg:LN polycrystalline powder with homogeneous Mg distribution, because few Mg atoms can diffuse into the LN lattices from the aggregated MgO particles. Furthermore, some MgO particles left in the as-synthesized LN powders due to the high melting temperature of MgO (3250 ± 20 K),³⁰ are detrimental to the crystal quality during the crystal growth. By improving the ball milling techniques or calcination process, researchers have tried to improve the homogeneity of Mg:LN powder, however, it is still a great challenge for the growth of Mg:LN and Mg doped near-stoichiometric LN (Mg:NSLN) crystal. It should be noted that solid-state reaction synthesis method for complex oxide polycrystalline powders often causes multi-phases in the product powder.²⁸ Contrary to the solid-state reaction, a wet chemical synthesis method is a promising method for the synthesis of multi-component oxides.^{31,32} It has many merits, such as better homogeneity, accurate composition control of the product powder, and lower reaction temperature. In recent years, synthesis of LN polycrystalline powders by the wet chemical method has been intensively investigated. As is well known, some

^aState Key Laboratory of Crystal Materials, Shandong University, Shandan Road, Jinan, 250100, China

^bYuanhong Technical Materials Ltd., Jining, China

^cDepartment of Electrical Engineering, Doshisha University, Kyotanabe, Kyoto 610-0321, Japan

commercial Nb–O compounds, such as Nb(OH)₅ and Nb₂O₅, do not readily form Nb ion solutions. To overcome this obstacle, niobium alkoxides have been used as Nb sources for synthesis of LN powders,³³ but the high cost of niobium alkoxides and their sensitivity to humidity limit their application in industry. Liu *et al.*³⁴ have synthesized LN powders by a solvothermal route and oxalic acid is used as a solvent. However, oxalic acid is harmful to human health and the environment. Recently, NbF₅ has been used for synthesis of LN powders.³⁵ Unfortunately, NbF₅ has certain inherent drawbacks due to its hygroscopicity and instability of chemical properties and needs special processing. In order to overcome the problems above, some innocuous organic acids (such as citric acid and DL-malic acid) have been utilized in the synthesis of niobium complexes.^{28,36,37} However, due to their low production this is still not suitable for industrial application. In the present work, a spray drying method was used to eliminate water from solution very rapidly instead of evaporation of the water in oven, which is suitable for industrial production. Most spray dried particles have spherical shape, uniform size and high flowability, which are favorable for single-crystal growth, especially for the continuous feeding double-crucible or a hanging crucible growth method for near-stoichiometric Mg:LN. In addition, this method can be applied to synthesis of other doped polycrystalline oxide powders for single-crystal growth or ceramic manufacture.

2. Experimental

2.1. Raw materials

Commercial niobium hydroxide (Nb(OH)₅ (Guangzhou Litop Non-ferrous Metals Co. Ltd, 99.99%), lithium carbonate (Li₂CO₃ Xin Jiang Research Institute of Non Ferrous Metals,

99.99%), magnesium oxide (MgO) (Sinopharm Chemical Reagent Co. Ltd 99.99%), and citric acid (CA, analytic grade, Sinopharm Chemical Reagent Co. Ltd) were used as the main reactants. Hydrogen peroxide (H₂O₂), ammonia solution (NH₃·H₂O) and electronic grade hydrochloric acid (HCl) (Sinopharm Chemical Reagent Co. Ltd) were also used in this experiment.

2.2. Sample preparation and single-crystal growth

The flowchart of the synthesis of Mg:LN polycrystalline powders is shown in Fig. 1. A certain amount of Nb(OH)₅ and HCl was allowed to react at 90 °C for 0.5 h. After cooling to room temperature naturally, some milky white colloid-like precipitate appeared and settled. After decanting off most of the residual HCl, the precipitate was dissolved by adding deionized water to form a transparent solution. NH₃·H₂O was added dropwise into the above solution to neutralize the acid in solution until the pH reached about 7. During this process a white flocculent precipitate appeared. After being washed 2–3 times with deionized water to remove residual HCl, citric acid was added into the precipitate and NH₃·H₂O was used to control the pH around 7. Finally, hydrogen peroxide (H₂O₂) was added into the above precipitate. After reaction for 30 min with agitation, the white precipitates dissolved leading to a yellow–green transparent solution.

At 90 °C, the reaction between Nb(OH)₅ and concentrated HCl occurs as follows: $2\text{Nb(OH)}_5 + 6\text{HCl} \rightarrow 2\text{NbClO}_3 + 8\text{H}_2\text{O}$

The NbClO₃ was hydrolyzed into a colloidal deposit of Nb₂O₅·nH₂O, which is easily dissolved in dilute hydrochloric acid. So the niobium ions can be dissolved while water was added. After adding citric acid (CA), the water-soluble Nb–CA complex was formed:

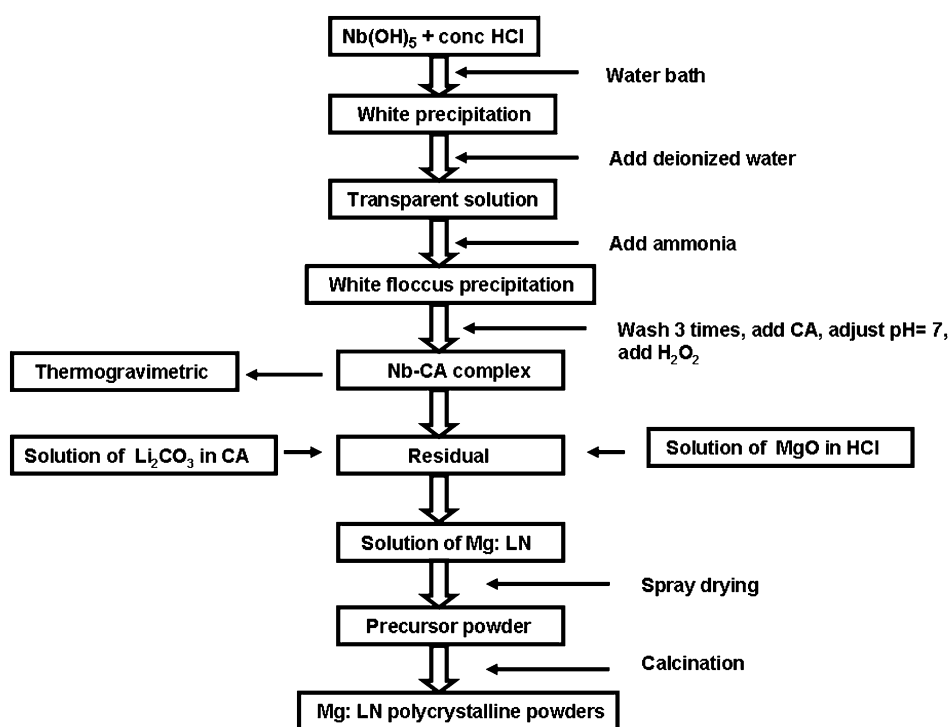


Fig. 1 Flowchart for preparing Mg:LN powder by wet-chemical/spray drying method.



The content of Nb_2O_5 in the solution was measured by thermogravimetric analysis (TGA). Li^+ and Mg^{2+} solutions were obtained by dissolving Li_2CO_3 and MgO in citric acid and hydrochloric acid, respectively. Finally, the three above solutions, Nb-CA solution, Mg-solution, and Li-solution, were measured according to the molar ratio of $\text{Li}/\text{Nb} = 48.6/51.4$ with 5 mol% of Mg^{2+} , and mixed thoroughly to form a transparent Mg:LN precursor solution.

The precursor solution was then spray dried by a laboratory scale spray dryer (SD-Basic, Labplant, UK). The experimental conditions were as following: temperature of air inlet = 190 °C, temperature of air outlet = 110 °C, pump speed = 0.45 L h⁻¹, air pressure = ca. 196 kPa. The Mg:LN precursor powder collected from the spray dryer was calcined at different temperatures (600, 720, 800 °C) for 2 h. In this work, precursor solutions with different concentrations of LN (#1, 0.2 mol L⁻¹; #2, 0.33 mol L⁻¹; #3, 0.58 mol L⁻¹) were prepared for comparison.

1 kg samples of Mg:LN powders synthesized by the above preparation method were used to grow Mg:LN. Mg:LN single crystals in air atmosphere by using the Czochralski technique.^{38,39} The Mg:LN powders were melted at 1250 °C and the time of heat preservation was about 2 h. The pulling and rotation speed was 0.8 mm h⁻¹ and 6.5 rpm, respectively.

2.3. Characterization

The precursor powder was characterized by thermogravimetry-differential thermal analysis (TG-DTA) (TG/DSC model: DSC-ZC, American PerkinElmer Company) in air from room temperature to 900 °C at a heating rate of 10 °C min⁻¹. The as-synthesized precursor and Mg:LN powder calcined at 600, 720 and 800 °C were characterized by X-ray powder diffraction (XRD, model: Bruker D8 Advance Cu-K α , $\lambda = 0.1540598$ nm (Ni-filtered), 40 kV, 40 mA) in 2θ from 15 to 80°. The infrared spectra (IR, model: NEXUS 670, American Thermo Nicolet company) of CA, precursor, and Mg:LN powder calcined at 720 or 800 °C for 2 h were measured in the range of 400–4500 cm⁻¹. The morphology of the as-synthesized precursor and Mg:LN powder with different samples was characterized by high-resolution scanning electron microscopy (SEM, model: Hitachi S-4800). The optical homogeneity and composition of the as-grown Mg:LN crystal was characterized by conoscopic interference using a laser interferometer (ZYGO GPI XP/D Zygo corporation), and ultraviolet absorption edge measurements.

3. Results and discussion

3.1. TG-DTA analysis

Thermogravimetry (TG) and differential thermal analysis (DTA) curves of Mg:LN precursor powders collected from a spray dryer are shown in Fig. 2. The TG curve reveals mass loss proceeds between 100 and 600 °C. The total mass loss is 80.76%. From DTA curve, the broad endothermic peak around 124 °C can be assigned as the release of combined water in powders according to the mass loss from room temperature to about 180 °C in the TG curve. The endothermic peak at about 257 °C in the DTA curve corresponding to the significant mass loss in TG indicates

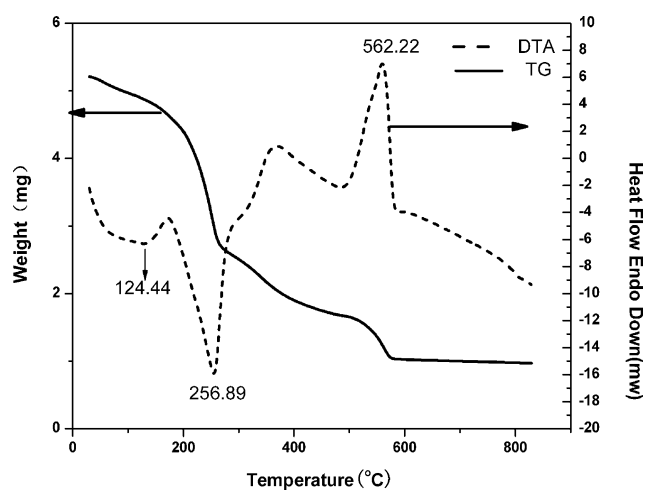


Fig. 2 TG and DTA curves of precursor powders.

the decomposition of citric acid and a small amount of NH_4Cl incorporated during the precursor preparation. The exothermic peak at 562.22 °C in the DTA curve indicates decomposition of the Nb-CA complex and crystallization. It is consistent with the mass loss in TG curve which is related to the organic combustion. From the TG curve, there is also a slow mass loss from 600 to 730 °C from a small amount of residual organics.

3.2. XRD analysis

Fig. 3 shows the XRD patterns of the precursor and samples calcined at different temperatures. Fig. 3a shows the XRD result of the precursor while Fig. 3b–d show XRD results of Mg:LN powders obtained after calcination at 600, 720 and 800 °C respectively. Fig. 3a shows no diffraction peaks appearing which indicates the absence of a crystalline phase in the precursor. After calcining at 600 °C, all the diffraction peaks were indexed by the structure of Mg:LN (JCPDS-83-1150) in Fig. 3b, which is consistent with the result of TG-DTA, indicating the crystallization process temperature around 600 °C. With calcination

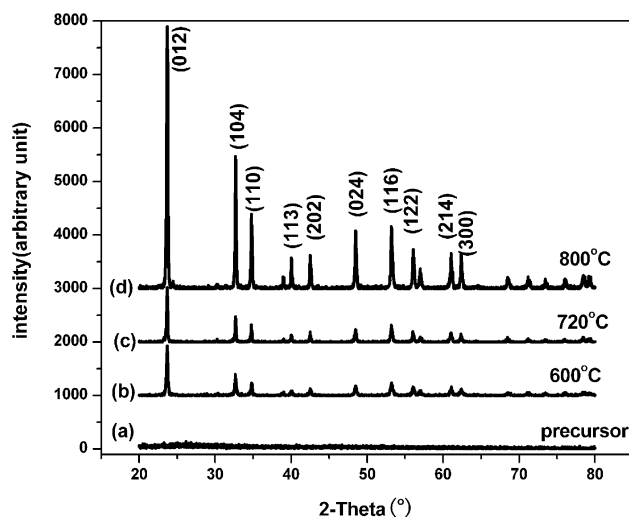


Fig. 3 X-Ray diffraction patterns of Mg:LN precursors (a) and the Mg:LN powder calcined at 600 °C (b), 720 °C (c) and 800 °C (d).

temperature increase, the diffraction peaks become sharper (Fig. 3c and d), which indicates an increase of degree of crystallization. The lattice constants of the as-synthesized Mg:LN powder were calculated according to the XRD data; they were determined as $a = 0.5153$ nm and $c = 1.3884$ nm, in good agreement with reference values, $a = 5.161$ Å and $c = 13.883$ Å (JCPDS-83-1150). Further, the values of a and c for the as-synthesized Mg:LN are higher than that of undoped congruent lithium niobate of $a = 0.5149$ nm and $c = 1.3862$ nm (JCPDS-20-631). The slight increase of lattice constants may be related to the doping of Mg^{2+} into the lattice of LN.

3.3. Infrared spectroscopy

The IR spectra of citric acid, Nb-CA complex, and Mg:LN powder calcined at 720 and 800 °C for 2 h are shown in Fig. 4.

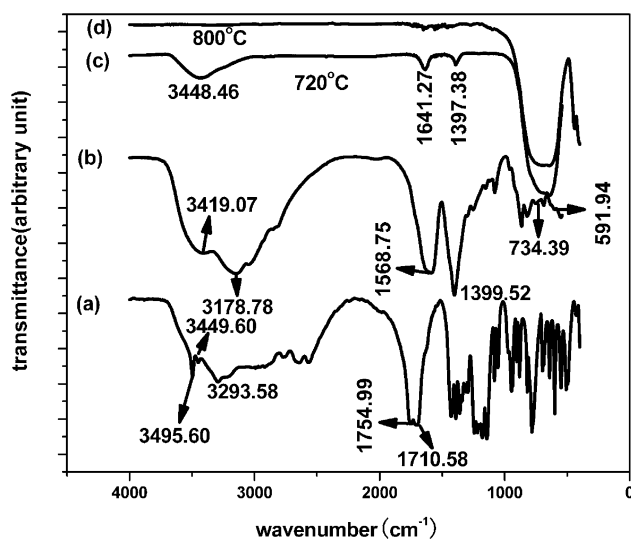


Fig. 4 IR spectra of the samples: citric acid (a), Nb-CA complex (b), Mg:LN powder calcined at 720 °C for 2 h (c), Mg:LN powder calcined at 800 °C for 2 h (d).

The IR spectrum of Nb-CA complex (Fig. 4b) is different from that of citric acid (Fig. 4a). The strong absorption peaks between 3600 and 2800 cm^{-1} are related to the O-H stretching vibration. However, the absorption peaks of the O-H stretching vibration in Fig. 4b show a red shift. This phenomenon indicates that chelation occurs between niobium ions and oxygen ions of OH^{-} in citric acid in the Nb-complex. Because oxygen atoms supply electrons to niobium atoms during the coordination, the electron cloud densities of O-H bonds decreases, which leads to lowering in energy of the stretching vibration and absorption peaks to shift toward lower wavenumber. The peak at 1710.5 cm^{-1} in Fig. 4a corresponds to the C=O stretching vibration, and it disappears in the Nb-CA complex (Fig. 4b). The absorption peaks at 591.9–734.4 cm^{-1} in Fig. 4b indicate the formation of Nb-O.^{40–42} All the remaining peaks of Fig. 4a are seen in Fig. 4b, which indicates that citric acid retains its molecular structure in the Nb-CA complex.

Since the organic compound (citric acid; CA) is used as chelating agent, carbon may be retained in the product calcined at lower temperature. Even in the IR spectra of Mg:LN calcined at 720 °C (Fig. 4c), some absorption peaks related to residual organics remain, such as peaks at 1641.3 and 1397.4 cm^{-1} , which are attributed to the stretching vibration of C=O and -COO- respectively. When the calcination temperature is increased to 800 °C, those absorption peaks vanish (Fig. 4d), and pure Mg:LN powder is obtained. This temperature is about 300 °C lower than the solid-state reaction temperature. The results of IR spectra are in accordance with XRD analysis, clearly suggesting use of a calcination temperature over 800 °C.

3.4. Morphology

Fig. 5 shows the morphology of the precursor and Mg:LN powder calcined at 800 °C. Fig. 5a–c show the morphology of the precursors spray dried from various solution concentrations (#1 0.2 mol L⁻¹; #2 0.33 mol L⁻¹; #3 0.58 mol L⁻¹, respectively) while Fig. 5d–f correspond to those of the as-calcined Mg:LN powders for samples #1, #2 and #3 obtained at 800 °C

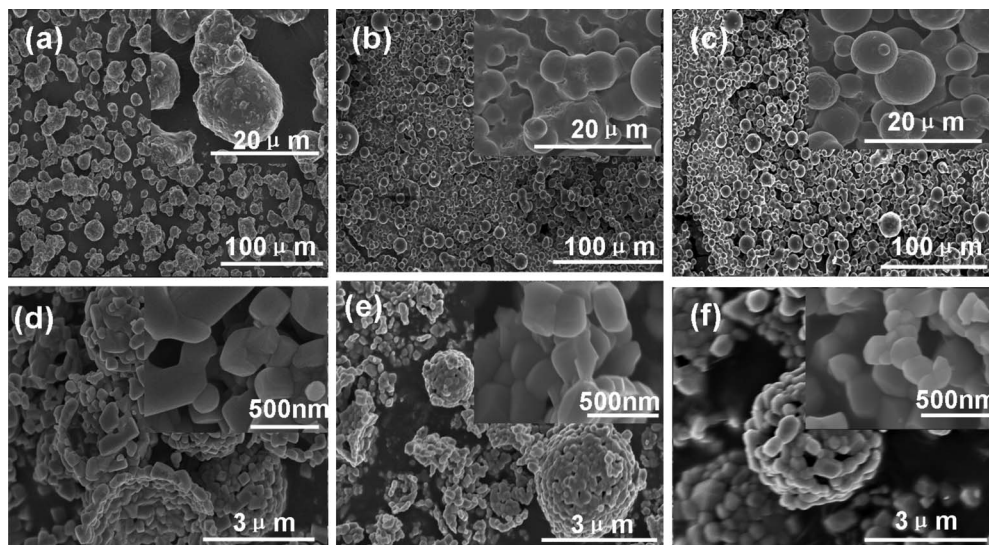


Fig. 5 SEM images of the precursor and Mg:LN powder at 800 °C : a, b and c correspond to the precursor spray dried from solutions #1, #2 and #3, respectively; d, e and f correspond to Mg:LN powders obtained from #1, #2 and #3 at 800 °C, respectively.

respectively. From Fig. 5a, it can be seen that the particles of precursor #1, obtained from solution with lowest concentration, have irregular shape with rough surface. From Fig. 5b, particles of precursor #2, obtained from higher concentration solution, adopt a spherical shape with sizes about 10 μm , but conglomeration occurs among the particles. As the concentration of the solution is further increased, the particles of precursor #3 are mostly spherical particles of about 5–10 μm in diameter and the surface of the particles is smoother than that from precursor #1 and #2. The reason for formation of spherical particle is that the surface tension of the precursor solution with high concentration is much higher than that of solutions at low concentration. Normally, larger surface tension of the solution easily causes spherical particle during the spraying process, and differences of concentration of the solutions is the main reason for obtaining different morphology of the precursor particles.

Fig. 5d–f show the detailed morphology of Mg:LN powders obtained from the related precursors #1, #2 and #3 by calcining at 800 $^{\circ}\text{C}$ for 2 h. All the Mg:LN samples consist of microparticles about 3 μm in diameter formed by self-assembled Mg:LN nanoparticles. For low solution concentration sample, sample #1, Mg:LN powders show some hollow spherical shell fragments of size about 3 μm , comprised of 200–500 nm nanoparticles (Fig. 5d). For higher solution concentration sample, sample #2, the spherical shells become more complete, and the nanoparticles on the shell are about 300–400 nm in size (Fig. 5e), which is smaller than those for sample #1. The Mg:LN powders prepared from highest solution are spheres with dense structure of 3 μm in diameter, which are comprised of small nanoparticles about 200–300 nm in size. The above results indicate that the concentration of precursor solution determines the size and morphology and microstructure of the precursor powder and the Mg:LN product powder calcined at 800 $^{\circ}\text{C}$. Higher concentration of precursor solution causes the formation of dense and spherical particles, which are attributed to the higher amount of solute in the solution and higher surface tension force. In addition, the size of the nanoparticles that assembles into the micropowder decreases with the increase of the solution concentration, which should decrease the melt temperature during the crystal growth.

3.5. Optical homogeneity of Mg:LN crystal

An Mg:LN single crystal (ϕ 55 \times 50 mm) was grown by using the above Mg:LN powder (sample #3) as a raw material. The crystal is complete without any defects such as, bubbles, inclusion, and obvious point defects. The optical conoscopic interference was taken for evaluation of optical homogeneity of the crystal. Fig. 6 shows a digital photo (a) and an optical conoscopic interference pattern (b) of the Mg:LN crystal. As is well known, the completeness of concentric interference rings and the symmetry of the black cross are measures of the completeness and optical homogeneity of the crystal. As shown in Fig. 6b, the interference rings are perfect, and the cross is symmetrical in all the parts of the crystal, which indicates that the crystal possesses very high optical homogeneity. To further confirm the optical quality of the crystal, the optical homogeneity data of the as-grown Mg:LN crystal and CLN (congruent LN) grown from solid-state reaction powder were obtained by laser interferometry (ZYGO GPI XP/D Zygo

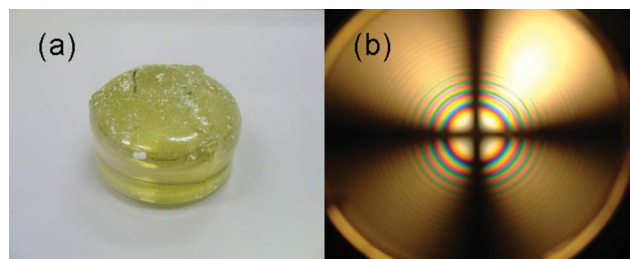


Fig. 6 Optical image (a) and optical conoscopic interference image (b) of the Mg:LN crystal grown from Mg:LN powder synthesized by the wet chemical-spray drying method.

corporation). The variations of refractive index (Δn) of Mg:LN is 2.02×10^{-5} , which is even lower than that of CLN (congruent LN), 8.67×10^{-5} . As is well known, MgO addition often causes non-homogeneity of LN, because of some defects or non-uniform distribution of Mg ions in the as-grown Mg:LN crystal. The Δn of as-grown Mg:LN was lower than that of the CLN, indicating the high homogeneity of MgO-doped LN powder.

3.6. Ultraviolet (UV) absorption edges of the Mg:LN crystal

For Mg-doped LN, the concentration of MgO of the crystal can be correlated to the UV absorption edge. To characterize the uniformity of distribution of MgO in the as-grown crystal, two wafers of 1.2 mm in thickness were cut from the top and tail of the crystal, and polished to optical grade. As shown in Fig. 7c three different sites on each wafer (marked as top-1, top-2, top-3 and tail-1, tail-2, tail-3, respectively) were chosen to measure the UV absorption edges and transmittance spectra by a Hitachi U-3500 spectrometer. Fig. 7a and b show the transmittance spectra and the UV absorption edges of the two samples respectively. As shown in Fig. 7a and b, the transmittance of the top and tail wafers is about 75%. Compared to the CLN, the UV absorption edge of Mg:LN is blue shifted to 313–314 nm, which is consistent of the results of Wengler⁴³ and Fan *et al.*⁴⁴ The absorption edges of top1–top3 and tail1–tail3 are located at 313.72, 313.74, 313.84, 314.31, 314.45 and 314.51 nm (with absorption coefficient 20 cm^{-1}) respectively. The differences of UV absorption edge is less than 1 nm in the whole crystal, which indicates the high optical homogeneity of the crystal.

Further characterizations and comparative investigation, especially the distribution homogeneity of Mg ions in Mg:LN single crystals grown from powders obtained by solid-state reaction and wet-chemical spray drying processes are underway. Because the method can overcome the problem of non-homogeneous distribution of MgO in polycrystalline Mg:LN powder, and can be used to mass produce Mg:LN single crystals, and especially because it eliminates MgO clution caused by residual MgO particles in LN polycrystalline powder synthesized by a solid-state reaction method, this method will have great application in the growth of high quality Mg:LN single crystals.

4. Conclusions

Mg:LN powders were successfully synthesized by using a wet-chemical-spray drying method. Homogenous and stable transparent Mg:LN precursor solutions can be obtained based on the reaction

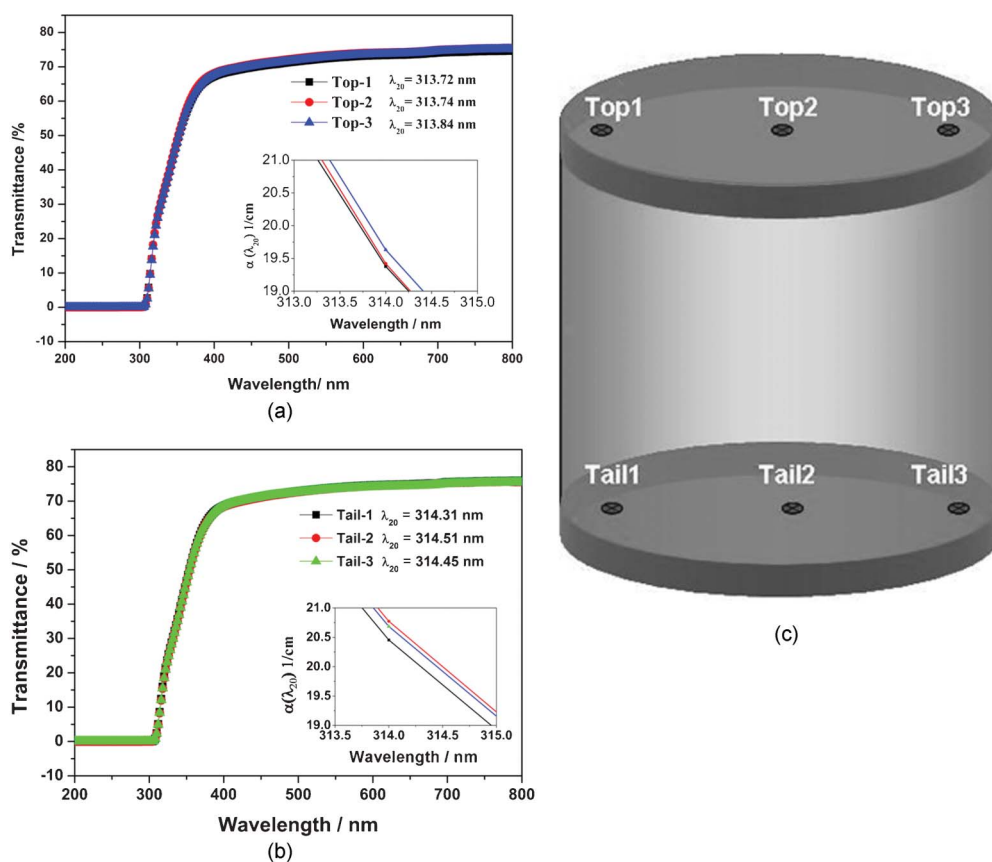


Fig. 7 UV absorption edges and transmittance spectra of top and tail wafers. Three different sites on each wafer (marked as top-1, top-2, top-3 and tail-1, tail-2, tail-3, respectively)

between $\text{Nb}(\text{OH})_5$ and HCl by adding citric acid to form a soluble Nb-CA complex. Spherical Mg:LN precursor particles can be collected by a spray drying method through controlling the concentration of precursor solution and spray drying conditions. Spherical Mg:LN microparticles constructed from Mg:LN nanoparticles were obtained at $800\text{ }^\circ\text{C}$, which is about $350\text{ }^\circ\text{C}$ lower than that of a conventional solid-state reaction synthesis method. Mg:LN powder synthesized through this method shows homogenous MgO distribution without any Li_2O loss. An optically homogenous Mg:LN single crystal has been grown using the Mg:LN powder through a conventional Czochralski technique without any adjustment. This synthesis method will have wide applications in Mg:LN, Mg:LiTaO₃ and other doped crystals due to its important advantages, such as use of commercially available chemicals, no special solvent, easy scale up and controllable stoichiometry.

Acknowledgements

This work was supported by the National High Technology Research and Development Program of China (863 Program No. 2006AA030106), NSFC (NSFDYS: 50925205, Grant: 50990303, IRG: 51021062), and the Program of Introducing Talents of Discipline to Universities in China (111 program No. b06015).

References

- 1 J. G. Bergmann, A. Askin, A. A. Ballman, J. M. Dziedzic, H. J. Levinstein and R. G. Smith, *Appl. Phys. Lett.*, 1968, **12**, 92.
- 2 F. Abdi, M. Aillerie, P. Bourson, M. D. Fontana and K. Polgar, *J. Appl. Phys.*, 1998, **84**, 2251.
- 3 J. R. Carruthers, G. E. Peterson and M. Grasso, *J. Appl. Phys.*, 1971, **42**, 1846.
- 4 I. Tomeno and S. Matsumura, *J. Phys. Soc. Jpn.*, 1987, **56**, 163.
- 5 B. C. Grabmaier, W. Wersing and W. Koestler, *J. Cryst. Growth*, 1991, **110**, 339.
- 6 S. Lamfredi and A. C. M. Rodrigues, *J. Appl. Phys.*, 1999, **86**, 2215.
- 7 T. Y. Chang, J. H. Jong and P. Yeh, *Opt. Lett.*, 1990, **15**, 743.
- 8 C.-T. Chen, D. M. Kim and D. von der linde, *Appl. Phys. Lett.*, 1979, **34**, 321.
- 9 F. Mok, M. Tackitt and H. M. Stoll, *Opt. Soc. Am. Tech. Dig. Ser.*, 1989, **12**, 74.
- 10 V. A. Fedorov, Y. N. Korkishko, G. Lifante and F. Cussó, *J. Eur. Ceram. Soc.*, 1999, **19**, 1563.
- 11 S. Breer and K. Buse, *Appl. Phys. B: Lasers Opt.*, 1998, **66**, 339.
- 12 E. Montoya, J. A. Sanz-Garcia, J. Capmany, L. E. Bausá, A. Dening, T. Kellner and G. Huber, *J. Appl. Phys.*, 2000, **87**, 4056.
- 13 P. Schlup, G. W. Baxter and I. T. Mckinnie, *Opt. Commun.*, 2000, **176**, 267.
- 14 R. S. Weis and T. K. Gaylord, *Appl. Phys. A: Solids Surf.*, 1985, **37**, 191.
- 15 H. K. Lam, J. Y. Dai and H. L. W. Chan, *J. Cryst. Growth*, 2004, **268**, 144.
- 16 E. Dogheche, V. Sadaune and X. Lansiaux, *Appl. Phys. Lett.*, 2002, **81**, 1329.
- 17 P. F. Bordui, R. G. Norwood, C. D. Bird and G. D. Calvert, *J. Cryst. Growth*, 1991, **113**, 61.
- 18 N. Iyi, K. Kitamura, F. Izumi, J. K. Yamamoto, T. Hayashi, H. Asano and S. Kimura, *J. Solid State Chem.*, 1992, **101**, 340.
- 19 G. Malovichko, V. Grachev and O. Schirmer, *Appl. Phys. B: Lasers Opt.*, 1999, **68**, 785.
- 20 F. P. Safaryan, R. S. Feigelson and A. M. Petrosyan, *J. Appl. Phys.*, 1999, **85**, 8079.
- 21 D. Xue, K. Betzler and H. Hesse, *Opt. Mater.*, 2001, **16**, 381.

-
- 22 K. C. Sweeney, L. E. Hulliburton, D. A. Bryan, R. R. Rice, R. Gerson and H. E. Tomaschke, *J. Appl. Phys.*, 1984, **45**, 805.
- 23 A. Kuroda and S. Kurimura, *Appl. Phys. Lett.*, 1996, **69**, 1565.
- 24 G. G. Zhong, J. Jian and Z. K. Wu, Proceedings of the 11th International Quantum Electronics Conference, IEEE Cat. No. 80, CH 61-0, June, 1980, p. 631.
- 25 D. A. Bryan, R. Gerson and H. E. Tomaschke, *Appl. Phys. Lett.*, 1984, **44**, 847.
- 26 V. T. Kalinnikov, O. G. Gromov, G. B. Kunshina, A. P. Kuz'min, E. P. Lokshin and V. I. Ivanenko, *Inorg. Mater.*, 2004, **40**, 411.
- 27 M. Liu and D. Xue, *Solid State Ionics*, 2006, **177**, 275.
- 28 E. R. Camargo and M. Kakihana, *Solid State Ionics*, 2002, **151**, 413.
- 29 C. D. E. Lakeman and D. A. Payne, *Mater. Chem. Phys.*, 1994, **38**, 305.
- 30 C. Ronchi and M. Sheindlin, *J. Appl. Phys.*, 2001, **90**, 3325.
- 31 V. Samuel, A. B. Gaikwad and A. D. Gadhav, *Mater. Lett.*, 2007, **61**, 765.
- 32 F. Zheng, H. Liu, D. Liu, S. Yao, T. Yan and J. Wang, *J. Alloys Compd.*, 2008, **77**, 688.
- 33 Z. Cheng, K. Ozawa, A. Miyazaki and H. Kimura, *Chem. Lett.*, 2004, **33**, 1620.
- 34 M. Liu and D. Xue, *Mater. Lett.*, 2005, **59**, 2908.
- 35 S. C. Navale, V. Samuel and V. Ravi, *Mater. Lett.*, 2005, **59**, 2476.
- 36 M. Liu, D. Xue and C. Luo, *J. Alloys Compd.*, 2006, **426**, 118.
- 37 S. Yao, F. Zheng, H. Liu, J. Wang, H. Zhang, T. Yan, J. Wu, Z. Xia and X. Qin, *Cryst. Res. Technol.*, 2009, **44**, 1235.
- 38 A. Rüber, in *Current Topics in Materials Science*, ed. E. Kaldis, North-Holland, Amsterdam, 1978, vol. 1, p. 481.
- 39 R. V. A. Murthy, K. S. Bartwal and K. Lal, *Mater. Sci. Eng., B*, 1993, **18**, L4.
- 40 E. Ruždić and N. Brničević, *Inorg. Chim. Acta*, 1984, **88**, 99.
- 41 K. Nakamoto, in *Infrared and Raman Spectra of Inorganic and Coordination Compounds, Part B: Applications in Coordination, Organometallic and Bioinorganic Chemistry*, Wiley, New York, 5th edn, 1997.
- 42 J. M. Jehng and I. E. Wachs, *Chem. Mater.*, 1991, **3**, 100.
- 43 M. C. Wengler, U. Heinemeyer and E. Soergel, *et al.*, *J. Appl. Phys.*, 2005, **98**(6), 064104.
- 44 Y. Fan, H. Li, F. Guo, Y. Xu and L. Zhao, *Opt. Commun.*, 2007, **278**, 413–417.